MAIN PARAMETERS OF MPD ELECTROMAGNETIC CALORIMETER IN LATEST GEOMETRY VERSION*

V.V. Kulikov, S.A. Bulychjov, M.A. Martemianov
M.A. Matsyuk, A.V. Skoblyakov

NRC "Kurchatov Institute" — ITEP, Moscow 117218, Russia

I.A. Tyapkin

Joint Institute for Nuclear Research, Dubna, MR 141980, Russia

A large cylindrical electromagnetic calorimeter is being built for the MPD/NICA detector. The final design of its supporting structure was recently approved. It greatly affected the design of the calorimeter itself and added a significant amount of passive materials. A program for geometric description of the calorimeter, taking into account the supporting structure, has just been developed by the ITEP team. In this report, the first Monte Carlo testing of this version of the calorimeter is presented and its main parameters are evaluated.

1. Introduction

The NICA project [1], implemented at the Joint Institute for Nuclear Research in Dubna, aims to study superdense nuclear matter, the properties of quark–gluon plasma and the mechanisms of transition of ordinary hadron matter to this new state. For this purpose, a heavy-ion collider with a maximum energy of $\sqrt{S_{NN}} = 11$ GeV and a Multi-Purpose MPD detector are under construction by the MPD international collaboration. The detector is based on a 900 ton cylindrical superconducting magnet with up to 5 kG magnetic field in a volume of 4 m in diameter and 7.4 m in length. Three main MPD subsystems are located in a magnetic field — a time-projection chamber, a time-of-flight detector and an electromagnetic calorimeter ECal. The latter will register photons and will identify electrons/positrons, which are one of the main probes for the formation of quark–gluon plasma.

---

* Presented at NICA Days 2019 and IV MPD Collaboration Meeting, Warsaw, Poland, October 21–25, 2019.

2. Electromagnetic calorimeter

ECal is placed in a cylindrical volume with an internal (external) diameter of 3.45 (4.6) and length of 6 m. It is assembled from 38 400 "shashlik"-type towers containing 210 alternating layers of 0.3 mm lead and a 1.5 mm scintillator, pierced by 16 WLS fibers to collect light on a 6×6 mm^2 silicon photomultiplier. At first, the tower is made as a $4 \times 4 \times 41.5$ cm^3 box, which is later machined to truncated trapezoid to densely fill the cylindrical volume and ensure that all axes of the towers are directed to the intersection point of the collider beams. Details of the ECal design and the current status of its construction are presented in [2]. The ECal simulation program of version v3, developed by the ITEP group, was described in [3]. Since the total weight of ECal towers is 60 tons, the development of the supporting structure has proved to be a very difficult task, which was recently successfully solved on the basis of modern technology using carbon fibers. The choice of this technology made it possible to provide the necessary strength with a minimum amount of passive materials in front of and inside the calorimeter. Around the circumference of the cylinder, ECal is divided into 25 sectors. Two baskets are inserted into each sector from opposite sides. Each basket has 6 rows of 8 modules each. The module contains two rows of 8 towers. Compared with the previous version v2 of the geometric description of ECal, which did not contain the supporting structure, the following passive materials have been added. In front of ECal is an internal support cylinder 25 mm thick of carbon fiber and 8 mm of the bottom of the fiberglass baskets. In total, they contribute to 12.7% of the radiation length. Inside the calorimeter, the carbon fiber walls between sectors 10 mm thick and the inner and outer 2 mm fiberglass walls of baskets were added. In total, these elements occupy 8% of the internal surface of ECal. It is clear that all these materials will lead to a deterioration in ECal parameters, but to what extent it will be shown in the next chapter.

3. ECal performance

ECal characteristics were determined by simulation using the Geant4 package in MPDRoot and FairSoft environment. Figure 1 shows the distribution of energy deposition in clusters for photons with an energy of 1 GeV differentially in the azimuthal angle ϕ of photon emission (Fig. 1 (a)) and integrally throughout the all calorimeter (Fig. 1 (b)). The distribution in Fig. 1 (b) has significant deviations from the Gaussian shape and a significant low-energy tail. This leads to the uncertainty in determining the parameters of the fit by the Gaussian distribution. Thus, fitting this distribution from energy corresponding to the level of 50 (30)% of the maximum at the low-energy side, the resolution is 5.0 (5.6)%, respectively. The main reason for both of these effects lies in the presence of longitudinal 2 mm
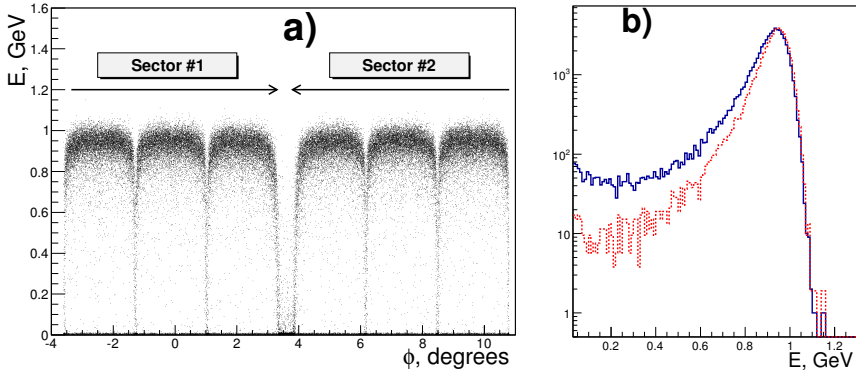
Fig. 1. (a) cluster energy for 1 GeV photons *versus* photon angle; (b) projection of (a) on Y-axis without and with the cut (see the text).

walls of baskets and 1 cm walls that divide sectors. These walls are clearly manifested in Fig. 1 (a). These effects can be reduced by excluding the zones near these walls. The dotted histogram in Fig. 1 (b) shows the result of such a selection, which improves the resolution from 5% to 4.5% and suppresses the low-energy tail about three times. Figure 2 shows the dependence of the energy resolution on the photon energy in the range from 50 to 3 000 MeV for both geometric versions with (v3) and without (v2 [4]) support structure. The parametrization $\mathrm{d}E/E = \sqrt{a^2/E + b^2}$ describes this energy dependence well. As expected, constant (b) is noticeably larger in v3, but the overall resolution drop is not large. Thus for 1 GeV, the resolution for v3 is 5%, and for v2 4.5%. It depends on the energy threshold for the towers. This dependence is shown in Fig. 2 (b). It can be seen that for 200 MeV photons, this dependence strongly affects the resolution, while for 1 GeV, this dependence can be neglected. In any case, the expected threshold of 5 MeV provides the maximum energy resolution. One of the most important tasks for ECal is the selection of electrons/positrons on the background of pions. Figure 3 allows making a simple estimation of this π/e suppression.
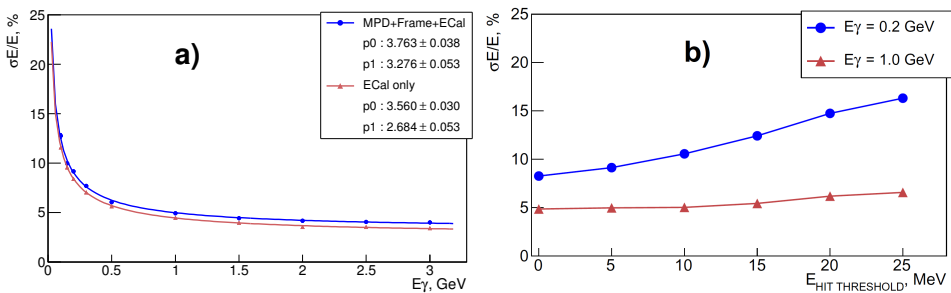
Fig. 2. (a) ECal energy resolution as a function of photon energy for v3 and v2; (b) its dependence on energy threshold for two photon energies.
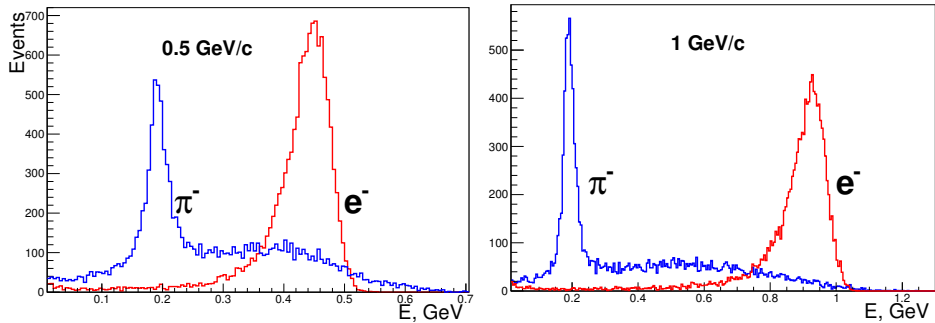
Fig. 3. Pion/electron separation for two momenta 0.5 and 1 GeV/c.

It shows the cluster energy for negative pions and electrons with momenta of 0.5 and 1 GeV/c. The electron peak is located at about 1 GeV, and pion peak near 200 MeV with a long high-energy tail due to nuclear interactions. Integrating the number of pions that deposit energy in the area under the electron peak, we can estimate the probability of a pion simulating an electron's energy deposition. Thus for the zone under the electron peak $\pm 2\sigma$, this probability is 7 (22)% for 1.0 (0.5) GeV/c respectively. These values have not changed much compared to version v2, where they were 5 (18)%. This change is simply due to a slight increase in the width of the electron peak in version v3. The same separation can be obtained also in version v3 with a slight loss in the efficiency of electron identification.

4. Conclusion

Despite a significant amount of passive materials in the ECal, its main parameters did not undergo significant changes. The energy resolution slightly deteriorated from 4.5% to 5% for photons with an energy of 1 GeV. The noticeable deviation of the energy deposition shape from the Gaussian and the presence of a low-energy tail causes some concern due to possible difficulties in developing methods for identifying clusters for high multiplicity events.

REFERENCES

[1] V.D. Kekelidze, *Phys. Part. Nucl.* **49**, 457 (2018).
[2] I.A. Tyapkin, Presented at the NICA Days 2019 and IV MPD Collaboration Meeting, Warsaw, Poland, October 21–25, 2019, not submitted to the proceedings.
[3] M.A. Martemianov *et al.*, *Acta Phys. Pol. B Proc. Suppl.* **14**, 533 (2021), this issue.
[4] B. Dabrowska *et al.*, *EPJ Web Conf.* **204**, 07015 (2019).